Bolometric Applications at Room Temperature

Chantal Gunther[1], Bruno Guillet[2], Fiény Kouadio[3], Jean-Marc Routoure[4], Laurence Méchin[5]

GREYC (CNRS-UMR 6072) ENSICAEN, University of Caen,

6 Boulevard Maréchal Juin - 14050 Caen cedex, France

[[1]chantal.gunther, [2]bruno.guillet, [3]fieny.kouadio, [4]jean-marc.routoure, [5]laurence.mechin]@greyc.ensicaen.fr

Abstract: In this work, $La_{2/3}Sr_{1/3}MnO_3$ (LSMO) thin films with high temperature coefficients have been chosen as thermometers for use in bolometric applications at room temperature and their temperature coefficient of resistance and noise characteristics were carefully measured. The Noise Equivalent Temperature (NET) value of 6.10^{-7} K/$\sqrt{\text{Hz}}$ at 10 Hz and 150 µA current bias for LSMO has been obtained in the 300 K - 400 K range. Our results are compared to literature and to other types of materials such as semiconductors (a-Si, a-Si:H, a-Ge, poly SiGe) and other oxide materials (semiconducting YBaCuO, VOx and other manganite compounds). The possible use of these thermometers with such low NET characteristics for the fabrication of both membrane-type bolometers for mid-infrared detection and antenna coupled bolometers for THz applications is discussed. Finally, we present the concept of a narrow band THz gas sensor, based on antenna-coupled bolometer.

Keywords: Low frequency noise, LSMO, uncooled bolometer, thermometer

1. INTRODUCTION

Bolometers are employed in a large variety of applications (space radiometry, optical communication, thermal imaging, spectroscopy, non contact temperature measurement…). The quite recent development of uncooled bolometers is of great interest for commercial applications, in particular, for infrared (IR) cameras. Nowadays, new classes of affordable and portable infrared cameras are commercially available. The range of applications for IR cameras is very large : vision under difficult conditions, (smoke, darkness), security, medical imaging, predictive maintenance…

For such applications, LSMO thin films present good properties (dR/dT, low noise) at 300 K. Their noise properties have been carefully investigated in order to specify the applications of LSMO thin films thermometers.

In section 2, we briefly review the operation principles of a resistive bolometer and explicit the noise contributions of a bolometer so as to present in section 3, the performances we obtained for our LSMO thermometers.

Section 4 gives a short analysis of the results compared to literature and makes an evaluation of the performances of both membrane-type bolometers for mid-infrared detection and antenna coupled bolometers for THz applications fabricated with these materials. Finally, we present the concept of a narrow band THz gas sensor, based on antenna-coupled bolometer.

2. PERFORMANCES OF A RESISTIVE BOLOMETER

The basic physics and performances of a bolometer based on a resistive thermometer are well established [1].

The detector consists of a radiation absorber of absorptivity η (black metal, antenna, cavity, feedhorn, etc...) and a thermometer R(T) that are connected to the heat sink via a heat link of thermal conductance G [W·K^{-1}] (figure 1).

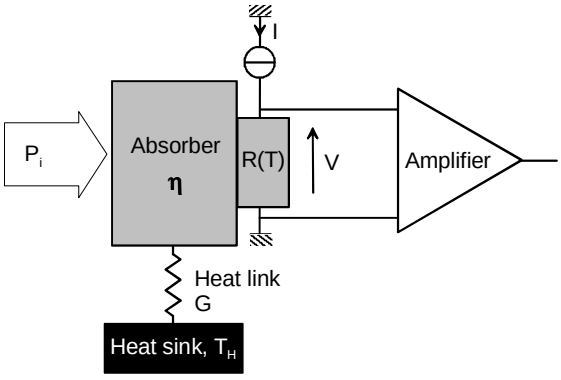

Fig. 1. Block diagram of a current biased (CCM) resistive bolometer coupled to the heat sink T_H via a thermal link G and readout electronics.

The resistive thermometer of real impedance R [Ω] is characterized by the temperature coefficient of resistance $\alpha = \frac{1}{R}\frac{dR}{dT}$ [K^{-1}] and the dimensionless coefficient $A = \frac{d(\ln R)}{d(\ln T)} = \alpha T$. The energy balance of a resistive bolometer operated in the Constant Current Mode (CCM) is:

$$C(T(t) - T_0) = \left[\eta P_i(t) + R[T(t)] \times I^2 - G \times [T(t) - T_H]\right] dt \quad (1)$$

for a small change in temperature. In this expression, C $[J.K^{-1}]$ represents the total heat capacity of the absorber and associated thermometer, $P_i(t)$ [W] the incident power, R(T(t)) [Ω] the thermometer resistance and I [A] the bias current. The time constant τ of the system is defined as: $\tau = C/G$.

2.1. Biasing modes of the resistive bolometer

Due to the electrical Joule power P_{el} of the bias current I, the thermometer equilibrium temperature T_0 [K] is higher than the heat sink temperature T_H [K] (T_H is assumed to be constant): $P_{el} = R(T_0)I^2 = G\times(T_0 - T_H)$. The responsivity $R_V(f) = \frac{\partial V}{\partial P}(f)$ [V/W] is given by:

$$R_V(f) = \frac{\eta\times I}{G_{eff}}\times\frac{dR}{dT}\times\frac{1}{1+j2\pi f\tau_{eff}} \quad (2)$$

G_{eff} and τ_{eff} are the effective conductance and time constant τ_{eff}: $G_{eff} = G - \alpha P_{el}$ and $\tau_{eff} = \frac{C}{G_{eff}}$.

The electrical Joule power P_{el} combined with the temperature coefficient α induces electrothermal feedback (ETF) [2,3]. The stability of the system depends on the sign of α and on the biasing mode. First, let us consider $\alpha > 0$ as in the LSMO case. In the constant current mode, the feedback coefficient L, defined as $L = \alpha P_{el}/G$, is positive and its value is limited to about 0.3 (<1) to avoid thermal runaway. In the Constant Voltage Mode (CVM), the electrothermal feedback is negative, there would be no limit for the bias voltage and the bolometer could be operated in a strong electrothermal feedback mode leading to a lower effective time constant $\tau_{eff} = \tau/(1+L)$. On the other hand, when $\alpha < 0$, CCM will give a negative ETF and CVM a positive ETF. Active negative electrothermal feedback mode made with an analog electronic feedback control would also improve bolometer performances [4,5].

2.2 Detection threshold of the resistive bolometer

The Noise Equivalent Temperature NET $[K/\sqrt{Hz}]$ corresponds to the smallest temperature fluctuation sensed by a thermometer (equivalent to the RMS temperature value in a 1-Hz bandwidth for a signal to noise ratio equal to one): $NET(f) = e_{ne}(f)/(\partial V/\partial T)$ with e_{ne}, the equivalent input voltage noise spectral density of the thermometer and the amplifier. NET(f) can also be expressed as:

$$NET(f) = \frac{T}{\sqrt{R}\times A\times\sqrt{P_{el}}}\times\sqrt{S_V(f) + 4k_BTR + e_n^2(f)} \quad (3)$$

where $S_V(f)$, $4k_BTR$ and $e_n^2(f)$ are respectively the thermometer low frequency excess noise, the thermometer Johnson noise (with k_B the Boltzmann constant) and the amplifier noise.

Eq. (3) shows that low NET values could be obtained if T and noise are low and A, R and P_{el} are high. T and A are usually determined by the choice of the material. It has to be noted that a high A value is often related to a narrow operating temperature range and that there is an upper limit in the choice of P_{el} in order to avoid parasitic self heating (or thermal runaway).

The main figures of merit of bolometers are the Noise Equivalent Power NEP $[W\cdot Hz^{-1/2}]$ and the specific detectivity D*. In the simple case where the photon and the phonon noise are negligible, the NEP can be written as the ratio of the voltage noise over the responsitivity, $NEP = e_{ne}/R_V$, which gives:

$$NEP(f) = NET(f)\times\eta^{-1}\times G_{eff}\times(1+j2\pi f\ \tau_{eff}) \quad (4)$$

The specific detectivity D^* $[cm\cdot Hz^{1/2}\cdot W^{-1}]$ is convenient for comparing bolometers of different sensing areas S $[cm^2]$ and will be used hereafter. It is defined as:

$$D^*(f) = S^{1/2}/NEP(f) \quad (5)$$

The background fluctuations noise-limited D^*_{BLIP} (Background Limited Infrared Photodetector) for an ideal bolometer having an emissivity of unity and viewing an angle of 2π steradians is independent of the receiving area but related to $(T_{bg}^5+T^5)^{-1/2}$ with T_{bg} the background temperature [K].

3. LOW NOISE LSMO BOLOMETERS

In the present work, we have chosen colossal magnetoresistive $La_{2/3}Sr_{1/3}MnO_3$ (LSMO) thin films with high temperature coefficients as thermometers for bolometric applications. LSMO has a Curie temperature of 350 K and can thus be operated around room temperature [6].

The LSMO thin films were deposited by pulsed laser deposition from a stoichiometric target onto $SrTiO_3$ (001) substrates. The laser energy density was 1-2 J/cm^2 (250 mJ), the target-to-substrate distance was 50 mm, the oxygen pressure was 0.35 mbar and the substrate temperature was 720 °C. These values were found optimal for producing single-crystalline films as judged by the X-Ray Diffraction (XRD) study. The latter indicated that the LSMO films were fully (001) oriented. The electrical resistivity of the unpatterned films is typically about 2 mΩ.cm at 300 K, which is close to the bulk value.

We have studied LSMO bridges with 3 different geometries which will be called large, medium and narrow of respective areas 400 μm × 96 μm, 660 μm × 35 μm and 660 μm × 6 μm. They were patterned by standard UV photolithography in 200 nm thick films. A four-probe noise measurement setup was used in order to reduce the influence of the contact resistance noise [7].

R(T) characteristics of the LSMO films are plotted in figure 2 for the 3 geometries [8]. At 300 K, the resistivity measured in the bridges was in the 0.5 – 2 mΩ.cm range and the α value was in the $1.2\ 10^{-2}$ - $1.4\ 10^{-2}$ K^{-1} range (giving A values in the 3.6 - 4.2 range).

The film voltage noise represented in figure 3 can be subdivided into 2 regions: a white noise part that corresponds to the Johnson noise of the thermometer expressed by $4k_BTR$ and a 1/f noise part, $S_V(f)$ which can be

described by the following Hooge empirical relation generally verified in normal metals:

$$\frac{S_V(f)}{R^2 I^2} = \frac{\alpha_H}{n \Omega f} \qquad (6)$$

where α_H, n, Ω and f are respectively the dimensionless Hooge parameter, the charge carrier density [m^{-3}], the sample volume [m^3] and the measuring frequency [Hz]. The low-frequency noise brings information about the film processing technique quality and the charge transport properties.

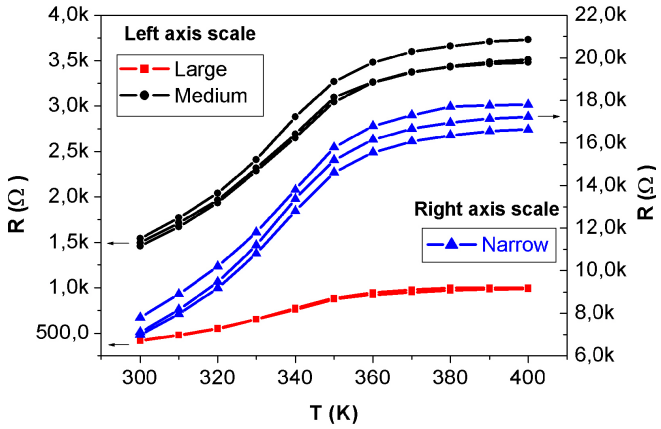

Fig. 2. Resistance versus temperature characteristics of bridges patterned in 200 nm-thick LSMO thin films for 3 different geometries [8].

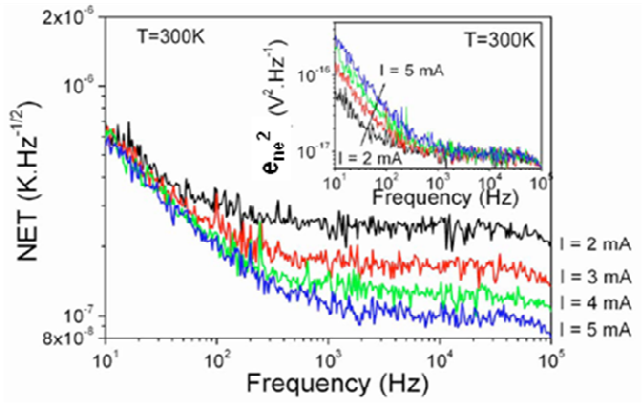

Fig. 3. Measured NET(f) of the 100 µm-wide, 300 µm-long line patterned in the 200 nm LSMO film on $SrTiO_3$ substrate for bias current in the 2 – 5 mA range at 300 K. Inset shows the corresponding e_{ne}^2(f).

In order to compare the noise level with other materials, we checked that Eq. (6) is valid and we deduced the normalized Hooge parameter α_H/n in the 10^{-31}-10^{-29} m^3 range in the whole measured temperature range for all the geometries. These values are among the lowest reported for LSMO thin films [9].

In the 300 - 400 K range, the lowest measured value of the NET was of 6 10^{-7} K·$Hz^{-1/2}$ at 10 Hz and 150 µA [10].

The absorption coefficient η has been measured and found to be equal to 0.85. The conductance G has been estimated to 10^{-3} W/K for the LSMO film on substrate [11] and corresponds to published datas. A conductance G of 10^{-6} W/K is expected for a membrane-type bolometer.

NEP(f) and D*(f) have been calculated for LSMO bolometers on substrate and on membrane for frequencies much smaller than $1/(2\pi\tau_{eff})$. Similar properties of LSMO films on substrate and on membrane have been assumed: film thickness e = 50 nm, detecting area = 50 x 50 μm^2, $\alpha_H/n = 10^{-29}$ m^3, ρ = 2 mΩ.cm, $\alpha = 0.02$ K^{-1}. The bias current of the thermometers has been fixed at $I = \sqrt{\frac{0,3G}{dR/dT}}$ with G = 10^{-3} W/K and 10^{-6} W/K for the LSMO films on substrate and membrane, respectively. As shown in figures 4(a) and 4(b), we could expect a NEP of a few pW/$Hz^{1/2}$ and a specific detectivity *D** around 10^9 cm·$Hz^{1/2}$·W^{-1} at 300 K and 30 Hz.

The studied thermometers are intended to be used in membrane-type bolometers for detection in the infrared (0.8 – 3 µm) to mid-infrared wavelength range (8 -14 µm). This wavelength range requires bolometers with relatively large area S since the condition $S\Omega_B > \lambda^2$ must be satisfied to avoid diffraction (Ω_B is the solid angle of the bolometer) [12]. Consequently, the heat capacity C, and thus the time constant τ, increase with the wavelength. The bolometer operates at relatively low frequencies and therefore the low frequency noise of such bolometers is an important parameter. Our low noise LSMO thermometers can thus play an important role in this wavelength range.

The LSMO thermometers will also be used in antenna-coupled bolometers on membranes for detection at higher wavelength (around 100 µm). The antenna is designed to couple the radiation into a transmission line which is terminated by a resistive thermometer. The size of this load must be much smaller than the wavelength so as to minimize the radiation losses of the load: it can be nanometric size, thus leading to small C and consequently small τ.

4. ANALYSIS AND PERSPECTIVES OF APPLICATION

Several reviews of heat-sensitive thin-film materials for room temperature thermometers have been published [13-14].

Representative examples for detection in the infrared wavelength at 300 K are listed hereafter. The highest possible D^*_{BLIP} (background fluctuations noise-limited) to be expected from a thermal detector operated at room temperature and viewing a background at the same temperature is 1.8×10^{10} cm·$Hz^{1/2}$·W^{-1}.

Amorphous silicon and amorphous hydrogenated silicon bolometers have shown a value of *D** of 3.2 10^8 cm·$Hz^{1/2}$·W^{-1} for a 70 × 70 μm^2 detecting area and 1.6 10^8 cm·$Hz^{1/2}$·W^{-1} for a 40 × 40 μm^2 detecting area, respectively. Amorphous germanium has also been used with *D**=4.7 10^8 cm·$Hz^{1/2}$·W^{-1} for a 70 × 70 μm^2 detecting area. Polycrystalline SiGe bolometers with optimal geometry are expected to present a specific detectivity of 1.5 10^{10} cm·$Hz^{1/2}$·W^{-1} for a 75 × 75 μm^2 detecting area [15].

The development of VOx bolometers has expanded and specific detectivities of 1.9 10^8 cm·$Hz^{1/2}$·W^{-1} at 30 Hz have

been obtained for a linear array of eight $10 \times 100\ \mu m^2$ elements [16]. Semiconducting YBCO thin film bolometers are also attractive since D^* as high as $1.3\ 10^8\ cm \cdot Hz^{1/2} \cdot W^{-1}$ at 30 Hz was estimated for a $50 \times 50\ \mu m^2$ suspended detector area [17]. Compared to manganites, the main disadvantages of the above materials are the large excess 1/f noise they present. We have shown (section 3) that a specific detectivity ten times higher should be achievable at 30 Hz and 300 K by 50 x 50 μm^2 LSMO bolometers on Si membrane with the geometric design we previously developed [18]. D* around $10^9\ cm \cdot Hz^{1/2} \cdot W^{-1}$ would be among the best reported results for manganite bolometers [19,20].

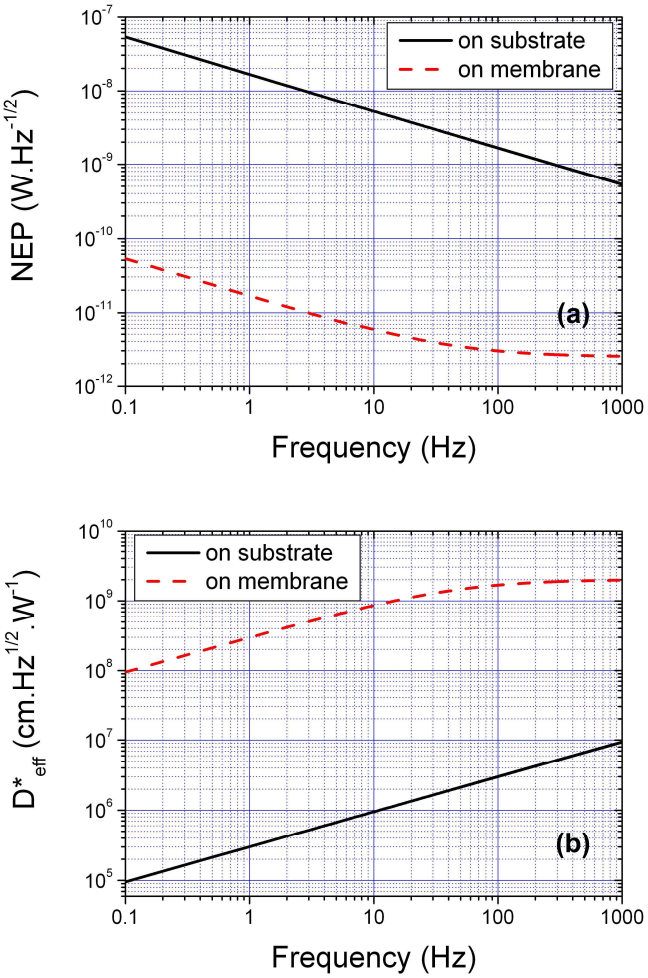

Fig. 4. LSMO bolometers on substrate and on membrane. Calculated NEP (a) and D_{eff}^* (b) vs frequency for T = 300 K, e = 50 nm, $\alpha_H/n = 10^{-29}\ m^3$, $\rho = 2\ m\Omega cm$, $\alpha = 0.02\ K^{-1}$, $G = 10^{-3}\ W.K^{-1}$ (LSMO on substrate) and 10^{-6} W. K^{-1} (LSMO on membrane), $e_n = 2\ nV.Hz^{1/2}$.

In case of a detection around or above the 100 µm wavelength, the electromagnetic coupling is made through a metallic antenna (antenna coupled composite bolometers). The incident power of the input wave is then partly transferred to the microload of the antenna. The load design requires both a high frequency matching to the antenna impedance and a low frequency matching for the heat exchanges between the microload and its surroundings. The main advantages of these antenna coupled bolometers lies in the heated volume which may be made very small. An important drawback is associated to losses in the dielectric and metallic parts of the device, reducing the coupling efficiency to about 20%. This problem can be reduced by a membrane technology that minimizes dielectric losses and ensures a good thermal insulation of the microload.

We intend to achieve a narrow band THz gas sensor, based on the antenna-coupled bolometer, for detecting Volatile Organic Compounds (VOCs): the sensor consists of a blackbody source, a gas cell, and a detector. The principle of operation comes from spectroscopy techniques which use the absorption spectrum to identify the chemical species. In our project, the blackbody radiation passes through the gas contained in the cell gas and the cell delivers the altered radiation to an array of detectors. Each detector is operated at one absorption line of the gas to be detected. The sensitivity of the detection and the ability to separate two adjacent lines requires narrow band detection. Usual planar antennas are broad band, so a high Q filter has to be inserted between the antenna and the filter as shown in figure 5.

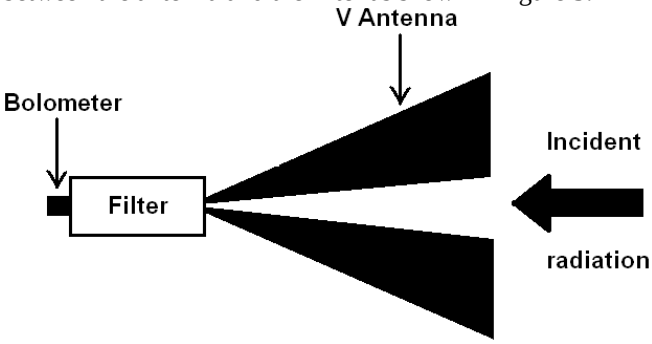

Fig. 5 Schematic of our narrow band THz gas sensor based on the antenna-coupled bolometer concept.

The growth of epitaxial LSMO thin films on silicon substrate combined with the membrane technology allows us to design a metallic antenna and a LSMO thermometer on membrane. A preliminary demonstrator is currently being developed at 115 GHz before extending it to the THz range

5. CONCLUSION

In conclusion, the presented LSMO thin films deposited onto (100) SrTiO3 have shown remarkable low 1/f noise, which could potentially enable the fabrication of high detectivity bolometers at room temperature. At last, antenna coupled bolometers are envisaged for wavelength around 100 µm to achieve a narrow band THz gas sensor.

REFERENCES

[1] P.L. Richards, *Bolometers for infrared and millimeters*, J.Appl. Phys. **76** (1), 1-24 (1994).

[2] K.D. Irwin, *An application of electrothermal feedback resolution particle detection,* Appl. Phys. Lett. **66** (15), 1998-2000 (1995).

[3] G.B. Brandao, L.A.L. de Almeida, G.S. Deep, A.M. Neff, *Stability conditions, nonlinear dynamics, runaway in microbolometers*, J. Appl. Phys. **90** (4), 1999-2008 (2001).

[4] M. Galeazzi, *An external electronic feedback system applied to a cryogenic μ-calorimeter*, Rev. Sci. Instr. **69** (5), 2017-2023 (1998).

[5] K. V. Ivanov, I. A. Khrebtov, and A. I. Stepanov, *Effect of active negative electrothermal feedback on the properties of high-temperature superconductor bolometers*, J. Opt. Tech. 71 (1), 51-54 (2004).

[6] A. Goyal, M. Rajeswari, R. Shreekala, S. E. Lofland, S. M. Bhagat, T. Boettcher, C. Kwon, R. Ramesh, T. Venkatesan, *Material characteristics of perovskite manganese oxide thin films for bolometric applications,* Appl. Phys. Lett. **71** (17), 2535-2537 (1997).

[7] J.M. Routoure, D. Fadil, S. Flament, L. Méchin, *A low noise high output impedance DC current source*, proceedings of the 19th International Conference on Noise and Fluctuations (ICNF 2007), Tokyo, Japan, Sept 2007

[8] L. Méchin, J.M. Routoure, S. Mercone, F. Yang, S. Flament, R. A. Chakalov, *1/f noise in patterned La2/3Sr1/3MnO3 thin films in the 300–400 K range,* J. Appl. Phys. **103**, 083709 (2008).

[9] P. Reutler, A. Bensaid, F. Herbstritt, C. Höfener, A. Marx, R. Gross, *Local magnetic order in manganite thin films studied by 1/f noise measurements*, Phys. Rev. B **62** (17), 11619-11625 (2000).

[10] L. Méchin, J.M. Routoure, B. Guillet, F. Yang, S. Flament, D. Robbes, R.A. Chakalov, *Low-noise La0.7Sr0.3Mn03 thermometers for uncooled bolometric applications*, J. Appl. Phys. **99**, 024903 (2006).

[11] L. Méchin, J.M. Routoure, B. Guillet, F. Yang, S. Flament, D. Robbes, R.A. Chakalov, *Uncooled bolometer response of a low noise $La_{2/3}Sr_{1/3}MnO_3$ thin film*, Appl. Phys. Lett. 87, 204103 (2005).

[12] P. Kruse, *Uncooled Thermal Imaging: Arrays, Systems, and Applications*, Vol. TT51, SPIE Press (June 2001).

[13] V.Y. Zerov. and V.G. Malyarov, *Heat-sensitive materials for uncooled microbolometers arrays*, J. Opt. Technol. **68** (12), 939-948 (2001).

[14] V.G. Malyarov, *Uncooled thermal IR arrays*, J. Opt. Technol. **69** (10), 750-760 (2002).

[15] S. Sedky, P. Fiorini, K. Baert, L. Hermans, R. Mertens, *Characterization and optimization of infrared poly SiGe bolometers*, IEEE Trans. Electron Dev. **46** (4), 675-682 (1999).

[16] C. Chen, X. Yi, J. Zhang, X. Zhao, *Linear uncooled microbolometer array based on VOx thin films*, Infrared Phys. Technol. **42,** 87-90 (2001).

[17] M. Almasri, Z. Çelik-Butler, D.P. Butler, A. Yaradanakul, A. Yildiz, *Uncooled multimirror broad-band infrared microbolometers*, J. Microelectromech. Syst. **11** (5), 528-535 (2002).

[18] L. Méchin, J.C. Villégier, G. Rolland, F. Laugier, *Double CeO2 /YSZ buffer layer for the epitaxial growth of YBa2Cu3O7-d films on Si (100) substrates*, Physica C **269,**124-130 (1996).

[19] J.H. Kim, S.I. Khartsev, A.M. Grishin, *Epitaxial colossal magnetoresistive $La_{0.67}(Sr,Ca)_{0.33}MnO_3$ films on Si*, Appl. Phys. Lett. **82** (24), 4295-4297 (2003).

[20] A. Lisauskas, S.I. Khartsev, A. Grishin, *Tailoring the colossal magnetoresistivity: $La_{0.7}(Pb_{0.63}Sr_{0.37})_{0.3}MnO_3$ thin-film uncooled bolometer*, Appl. Phys. Lett. **77** (5), 756-758 (2000).